[17] M. S. Shur, "Analytical model of GaAs MESFET's," *IEEE Trans. Electron Devices*, vol. ED-25, no. 6, pp. 612–618, June 1978.
[18] ——, "Low field mobility, effective saturation velocity and performance of submicron GaAs MESFET's," *Electron. Lett.*, vol. 18, no. 21, pp. 909–911, Oct. 1982.
[19] C. M. Snowden and R. Pantoja, "Quasi-two-dimensional MESFET simulation for CAD," *IEEE Trans. Electron Devices*, vol. 36, no. 9, pp. 1564–1573, Sept. 1989.
[20] M. Ali Khatibzadeh and R. J. Trew, "A large-signal, analytical model for the GaAs MESFET," *IEEE Trans. Microwave Theory Tech.*, vol. 36, pp. 231–238, Feb. 1988.
[21] C. S. Chang *et al.*, "GaAs MESFET analytic theory for current-voltage characteristics and field distribution," *IEEE Trans. Electron Devices*, vol. ED-36, no. 2, pp. 281–288, Feb. 1989.
[22] A. Cappy *et al.*, "Noise modeling of submicrometer-gate two-dimensional electron-gate field-effect transistor," *IEEE Trans. Electron Devices*, vol. ED-32, no. 12, pp. 2787–2796, Dec. 1985.

Fullwave Analysis of Planar Microwave Circuits by Integral Equation Methods and Bilinear Transformations

Andreas Janhsen, Burkhard Schiek and Volkert Hansen

***Abstract*—Planar microwave circuits are simulated by a mixed space-spectral domain integral method which allows the consideration of space-varying impedances. For an efficient computation of scattering parameters of circuits containing lumped elements within this full wave analysis, a bilinear transformation is used. Furthermore, by this so-called Möbius transformation it is possible to decide whether an impedance region of finite size can be interpreted as a lumped element or not.**

I. Introduction

Since the early 80's there is an increasing interest in the investigation of planar microwave circuits based on a numerical solution of Maxwell's equations. These methods can be roughly devided into two groups:

The simulation of microwave circuits by finite differences (e.g., [1]), finite elements (e.g., [2]), by the transmission line method (e.g., [3]) and similar methods is advantageous for circuits with complicated shapes, because these techniques are based on a three-dimensional discretisation of the metallization of the circuit as well as of the dielectric structure. Lumped impedance elements, space varying conductivity and a finite thickness of the metallisation can be considered. However, an enormous numerical expense is necessary because of discretising in all three dimensions. Thus, these methods are mainly used for circuit simulations where the dimensions of the geometry are in the range of a wavelength. Radiation of the circuit into free space can only be considered approximately.

The second group includes the integral equation techniques (e.g., [4]–[6]) and in the broadest sense the method of lines [7]. Here, the three-dimensional discretization is reduced to a two-dimensional one. Therefore, the dielectric layers are described by their Green's function. The expenditure of analytical and program-technical preparation yields an efficient computation of the circuits for which the assumption of a plane layered dielectric environment is valid. Defining ideal electric or magnetic sidewalls surrounding the circuit, FFT algorithms (e.g. [8]) can be used advantageously. Finite conductivity and a finite thickness of the metallisation can be considered approximately defining a surface impedance. A method for the simulation of active and/or passive lumped elements within the integral equation techniques is described in [9]. This approach can be generalized to space-varying surface impedances [10].

The latter will be discussed in this paper. First a general model for circuits embedded in layered dielectric media will be introduced. Subsequently an integral equation technique of planar microwave circuits including space varying surface impedances is shortly outlined. The correlation of port-quantities, e.g., scattering parameters, and circuit terminals, e.g., lumped impedances, is created with the help of a bilinear transform. This leads to an efficient computation of scattering parameters of circuits containing lumped elements. Furthermore, it becomes possible to give a measure for the numerical validity of calculated scattering parameters and an indicator is definable, by which it can be decided whether an impedance region of finite size can be interpreted as a lumped element or not. By several examples the efficiency of this method is illustrated.

II. Model and Integral Equation

The multiport circuit which is to be analyzed is embedded in a layered dielectric medium (Fig. 1). By this model not only microstrip circuits with or without a superstrate but also stripline, coplanar and similar structures can be examined.

The surface current density $\vec{J}(x, y)$ on the metallic structure is represented by a sum over N piecewisely defined basis functions $f_n(x, y)$ with current amplitudes I_n:

$$\vec{J}(x, y) = \sum_{n}^{N} I_n \frac{f_n(x, y)}{b_n} \vec{u}_n, \tag{1}$$

where b_n is the width of the nth current mode. The number of basis functions depends on the complexity of the circuit.

The electric field has to fulfill the surface impedance boundary condition on the circuit (see e.g. [11]):

$$\vec{E}(x, y)|_{\tan} = Z_{\text{tot}}(x, y)\vec{J}(x, y) + \vec{E}^{\text{ex}}|_{\tan}. \tag{2}$$

The space-varying surface impedance consists of two parts

$$Z_{\text{tot}}(x, y) = Z_c + Z(x, y). \tag{3}$$

Thus, in addition to a finite conductivity Z_c which represents the overall conductor losses, we have a space-varying surface impedance $Z(x, y)$. By this space-varying surface impedance different kinds of metallisation can be modeled (e.g. a superconductive film) or/and we can model impedances of finite size or infinite small size. Introducing a Green's function of the stratified dielectric structure an integral equation can be obtained which is formulated in the spectral-domain as well as in the space-domain [9], [10]. Applying the method of moments we get the following set of linear equations:

$$\sum_{i}^{N} I_i(Z_{ji} - Z_{ji}^{xy}) = V_j \quad \text{with} \quad j = 1, \cdots, N + L. \tag{4}$$

$$Z_{ji} = \frac{1}{4\pi^2} \int_{k_y} \int_{k_y} \vec{u}_j (\overleftrightarrow{G}(k_x, k_y) - Z_c \overleftrightarrow{I}) \vec{u}_i \cdot \frac{F_i(k_x, k_y) F_j^*(k_x, k_y)}{b_i b_j} dk_x\, dk_y, \tag{5}$$

Manuscript received August 13, 1991; revised March 6, 1992.
The authors are with the Institut für Hochfrequenztechnik, IC6/134, Ruhr-Universität Bochum, 4630 Bochum, Germany.
IEEE Log Number 9200459.

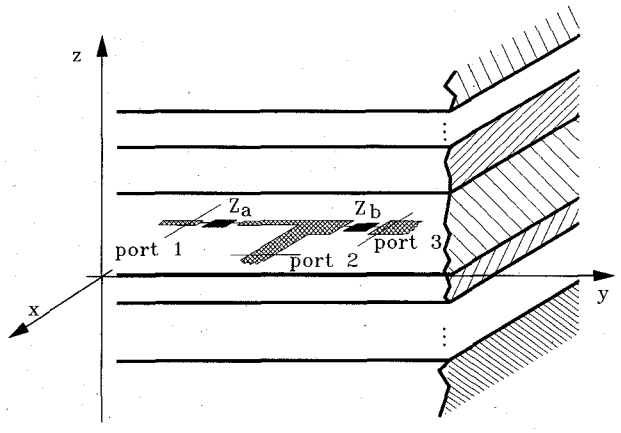

Fig. 1. Planar multiport circuit in a layered dielectric medium (example).

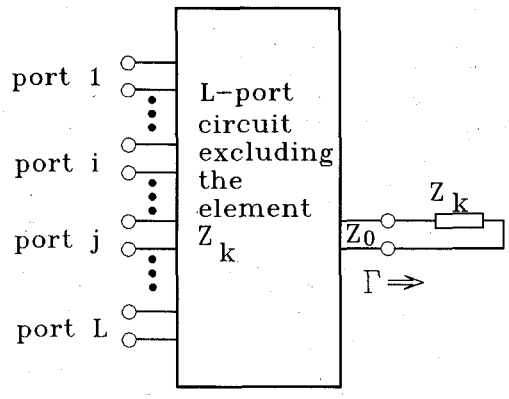

Fig. 2. L-port circuit excluding the element Z_k.

$$Z_{ji}^{xy} = \int_x \int_y \vec{u}_j \vec{u}_i Z(x, y) \frac{f_i(x, y) f_j(x, y)}{b_i b_j} dx\, dy. \tag{6}$$

$F(k_x, k_y)$ is the Fourier transform of the basis function $f(x, y)$, $\overleftrightarrow{G}(k_x, k_y)$ is the Fourier transform of the Green's function $\overleftrightarrow{G}(\vec{r}, \vec{r}\,')$. V represents the excitation of the circuit and will not be discussed here.

In most cases, the calculation of the elements Z_{ji} and V_j is very time consuming. In contrast to this, the matrix elements Z_{ji}^{xy} can be obtained analytically. A variation of the space-varying impedance changes only the elements Z_{ji}^{xy} and the matrix equation can be rewritten easily. The only time consuming part remains in solving the linear equations. Nevertheless, for large matrices and/or many different values of the lumped elements, this method is often too slow. Therefore in the next part, a bilinear transformation is used, by which the computation time can be reduced substantially.

III. The Bilinear Transformation

Microwave circuits are mainly characterized by their scattering parameters (port quantities). Lumped elements like impedances are to be seen as terminal quantities because only by this formulation an impedance can be written as the quotient between a voltage and a current.

For an arbitray L-port (Fig. 2) the relation between scattering parameters of the ports j and i on one side and the k's terminal element Z_k of the circuit on the other side is deduced from a bilinear transformation [12]. Usually, this so called Möbius transformation is used for "large scale sensitivity analysis" of networks in terms of currents, voltages and impedances, but as shown in the following text it is also applicable to the calculation of scattering parameters obtained by the solution of the integral equation (4): Defining the terminal k as an auxiliary port, the reflection coefficient Γ of this port is connected with the scattering parameter S_{ij} by

$$S_{ij} = \frac{a\Gamma + b}{c\Gamma + 1}. \tag{7}$$

By the substitution

$$\Gamma = \frac{Z_k - Z_0}{Z_k + Z_0} \tag{8}$$

we get

$$S_{ij} = \frac{a' Z_k + b'}{c' Z_k + 1}. \tag{9}$$

Thus, we have a relation between the terminal element Z_k and the scattering parameter S_{ij}.

For complex quantities related by the Möbius transformation one can deduce the following invariance property of the double-cross-ratio ([13]):

$$\frac{(S_{ij}^{(1)} - S_{ij}^{(2)})(S_{ij}^{(3)} - S_{ij}^{(4)})}{(S_{ij}^{(1)} - S_{ij}^{(4)})(S_{ij}^{(3)} - S_{ij}^{(2)})} = \frac{(Z_k^{(1)} - Z_k^{(2)})(Z_k^{(3)} - Z_k^{(4)})}{(Z_k^{(1)} - Z_k^{(4)})(Z_k^{(3)} - Z_k^{(2)})}. \tag{10}$$

Thus, (10) connects $m = 1, \cdots, 4$ values of scattering parameters $S_{ij}^{(m)}$, which describe the electromagnetic behavior between the ports j and i, with $m = 1, \cdots, 4$ values of the lumped element $Z_k^{(m)}$ of the kth terminal. For the variation of the value of a single lumped element $Z_k = Z_k^{(4)}$ of a circuit, one has to calculate the scattering parameters for three different values of this lumped element by the matrix equation (4). For each additional value of the lumped element Z_k the scattering parameter S_{ij} can simply be obtained using

$$S_{ij} = \frac{S_{ij}^{(3)}(S_{ij}^{(1)} - S_{ij}^{(2)})(Z_k^{(1)} - Z_k)(Z_k^{(3)} - Z_k^{(2)}) - S_{ij}^{(1)}(S_{ij}^{(3)} - S_{ij}^{(2)})(Z_k^{(1)} - Z_k^{(2)})(Z_k^{(3)} - Z_k)}{-(S_{ij}^{(3)} - S_{ij}^{(2)})(Z_k^{(1)} - Z_k^{(2)})(Z_k^{(3)} - Z_k) + (S_{ij}^{(1)} - S_{ij}^{(2)})(Z_k^{(1)} - Z_k)(Z_k^{(3)} - Z_k^{(2)})} \tag{11}$$

which follows from (10). It is remarkable that even the scattering parameters given by this procedure are solutions of the electromagnetic boundary problem and take e.g. the radiation of the circuit into consideration.

Solving (4) for $m = 1, \cdots, 4$ different values for the kth impedance $Z_k^{(m)}$ one can establish two simple numerical tests for scattering parameters:

- For a structure which contains lumped elements, (10) must be fulfilled exactly. Thus such a structure and (10) can be used to check roughly the accuracy of a numerical solution via the following:

$$a = \frac{(S_{ij}^{(1)} - S_{ij}^{(2)})(S_{ij}^{(3)} - S_{ij}^{(4)})}{(S_{ij}^{(1)} - S_{ij}^{(4)})(S_{ij}^{(3)} - S_{ij}^{(2)})}$$

$$b = \frac{(Z_k^{(1)} - Z_k^{(2)})(Z_k^{(3)} - Z_k^{(4)})}{(Z_k^{(1)} - Z_k^{(4)})(Z_k^{(3)} - Z_k^{(2)})}$$

$$D(S_{ij}) = \left| 1 - \frac{a}{b} \right| \doteq 0. \tag{12}$$

- Using numerical calculations which are known to be precise it can be determined by (12), whether a circuit element can be taken as a "lumped element" or not. In other words, whether the dimensions are "small" compared to the wavelength. Detailed investigations show, that for impedances in the range up to $|Z| = 100\ \Omega$ a value of $D(S_{ij}) < 0.1$ leads to a phase error of less than 13° and an error in the magnitude of less than 4% compared to the scattering parameters of lumped elements.

IV. Applications to Microstrip Circuits

The definition of a lumped element of microstrip circuits requires that the geometric dimensions of a terminal must not result in a phase shift. Thus, neglecting the transverse current distribution, for microstrip lines a terminal can be defined by a *line* transverse to the current.

The application of the cross-ratio (10) to scattering parameters for a variation of the value of one terminal element is illustrated by the example of a microstrip line with a series impedance Z (Fig. 3). We distinguish between two cases: For an impedance Z in the range from 0 Ω to 600 Ω the scattering parameters S_{11}^{mat} are calculated using (4), first. For a second calculation of S_{11} we take the values

$$S_{11}^{\text{mat}}(Z^{(1)} = 10\ \Omega),\ S_{11}^{\text{mat}}(Z^{(2)} = 150\ \Omega) \quad \text{and} \quad S_{11}^{\text{mat}}(Z^{(3)} = 500\ \Omega)$$

and obtain the scattering parameters $S_{11}^{\text{möb}}$ for all other values of Z simply by (11). Fig. 3 shows the difference $|S_{11}^{\text{mat}} - S_{11}^{\text{möb}}|$ for two impedance regions of different length s. For a line impedance ($s = 0$) (equivalent to a lumped element) the differences between the results obtained by the matrix equation (4) and by the Möbius transform (11) are in the range of 10^{-7} and can be neglected (Fig. 3 solid line, enlarged by 5000). But even for a small length of the impedance region ($s = 0.2$ mm) the accuracy of the scattering parameters obtained by (11) is better than 10^{-3}. For these calculations the surface impedances $Z_{\text{surf}}^{(i)}$ have been chosen in such a way, that the overall impedance of the region is equal to the value of the line impedance, that means

$$Z_{\text{surf}}^{(i)} = Z^{(i)}\,\frac{w}{s}. \tag{13}$$

For a length of $s = 0.4$ mm the error increases by 100% (not shown in Fig. 3).

In a further calculation the relation between the length of s of an impedance region and the error which results using (11) is investigated by (12). The geometry is identical to Fig. 3. For impedances $Z^{(1)} = 50\ \Omega$, $Z^{(2)} = 250\ \Omega$, $Z^{(3)} = 500\ \Omega$ and $Z^{(4)} = \infty\Omega$ —the latter is simulated by a gap— $D(S_{11})$ and $D(S_{21})$ are shown in Fig. 4 as a function of the length s. In order to get comparable results again the used surface impedance is chosen according (13). Note that the crosstalk across the gap is considered solving the electromagnetic boundary problem. The increasing error for an increasing length of the impedance region is rather obvious. This means, that the assumption of lumped elements, the Möbius transformation is based on, fails for an increasing length s and the circuit impedance has no longer the electromagnetic behaviour of a lumped element.

Fig. 5 shows the scattering parameter S_{11} of an asymmetric T-junction. For a variation of the value of a line impedance Z in the range from 0–200 Ω the best matching is obtained for $Z = 17$ Ω. This calculation is based on the scattering parameters

$$S_{11}^{\text{mat}}(Z^{(1)} = 0\ \Omega),\ S_{11}^{\text{mat}}(Z^{(2)} = 150\ \Omega) \quad \text{and} \quad S_{11}^{\text{mat}}(Z^{(3)} = 500\ \Omega). \tag{14}$$

For all other values of the impedance Z equation (11) is used.

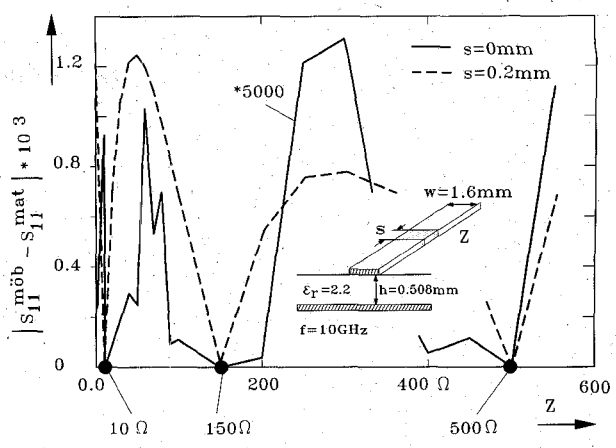

Fig. 3. Difference between scattering parameters obtained by (4) and (11).

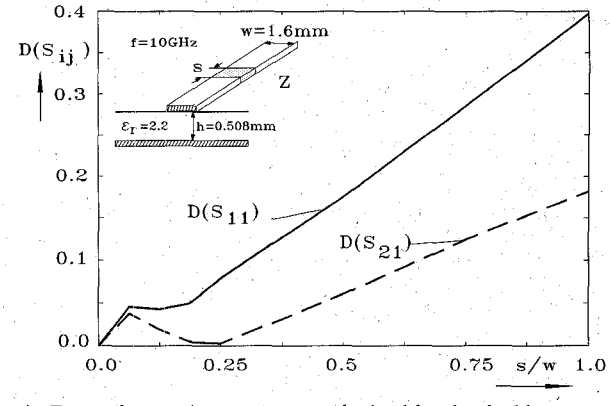

Fig. 4. Error of scattering parameters obtained by the double-cross-ratio (10) caused by an impedance region of finite size (see (12)).

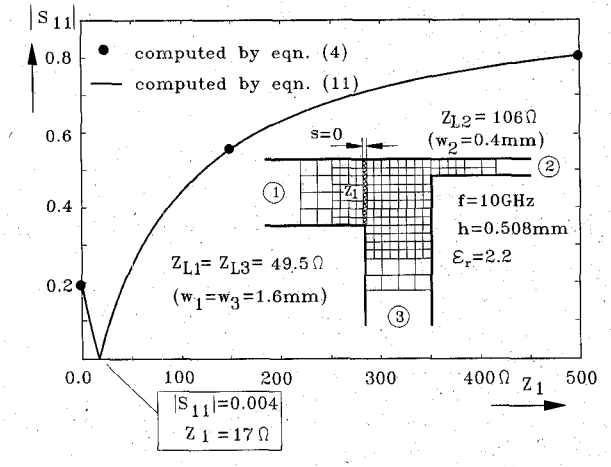

Fig. 5. Reflection of a asymmetrical T-junction for a variable impedance Z_1.

Acknowledgment

The authors wish to thank Dipl. Ing. R. Kulke who carried out a lot of the computations.

References

[1] X. Zhang and K. K. Mei, "Time-domain finite difference approach to the calculation of the frequency-dependent characteristics of microstrip discontinuities," *IEEE Trans. Microwave Theory Tech.*, vol. 36, pp. 1775–1787, 1988.

[2] J.-F. Lee, "Analysis of passive microwave devices by using three-dimensional tangential vector finite elements," *Int. J. Numerical Modelling: Elec. Netw., Dev. and Fields*, vol. 30, pp. 235–246, 1990.

[3] P. B. Johns, "A symmetrical condensed node for the TLM method," *IEEE Trans. Microwave Theory Tech.*, vol. MTT-35, pp. 370–377, 1987.

[4] R. H. Jansen, "The spectral-domain approach for microwave integrated circuits," *IEEE Trans. Microwave Theory Tech.*, vol. 33, pp. 1043–1056, 1985.

[5] R. W. Jackson, "Full wave, finite element analysis of irregular microstrip discontinuities," *IEEE Trans. Microwave Theory Tech.*, vol. 37, pp. 81–89, 1989.

[6] W. P. Harokopus and P. B. Katehi, "Characterization of microstrip discontinuities on multilayer dielectric substrates including radiation losses," *IEEE Trans. Microwave Theory Tech.*, vol. 37, pp. 2058–2065, 1989.

[7] S. B. Worm and R. Pregla, "Hybrid-mode analysis of arbitrarily shaped planar microwave structures by the method of lines," *IEEE Trans. Microwave Theory Tech.*, vol. MTT-32, pp. 191–196, 1984.

[8] R. H. Jansen and J. Sauer, "High-speed 3D em simulation for MIC/MMIC CAD using the spectral operator expansion (SOE) technique," *IEEE MTT-S Microwave Symp. Dig.*, Boston, 1991, pp. 1087–1090.

[9] A. Janhsen and V. Hansen, "Spectral analysis of multiport microstrip circuits with active and passive lumped elements," in *20th EUMC Rec.*, Budapest, Hungary, 1990, pp. 1053–1058.

[10] ——, "Modeling of planar circuits including the effect of space-varying surface impedances," *IEEE Microwave Guided Wave Lett.*, vol. 1, pp. 158–160, July 1991.

[11] J. M. Pond, C. M. Krowne, and W. L. Carter, "On the application of complex resistive boundary conditions to model transmission lines consisting of very thin superconductors," *IEEE Trans. Microwave*, vol. 37, 1989, pp. 181–190.

[12] R. K. Brayton and R. Spence, *Sensitivity and Optimization*. Amsterdam-Oxford-New York: Elsevier: 1980.

[13] T. E. Rozzi, J. H. C. van Heuven, and A. Meyer, "Linear networks as Möbius transformations and their invariance problems," *Proc. IEEE*, vol. 59, no. 5, pp. 802–803, 1971.

A High Frequency Model Based On The Physical Structure Of The Ceramic Multilayer Capacitor

L. C. N. de Vreede, M. de Kok, C. van Dam, and J. L. Tauritz

***Abstract*—In this paper modelling of the high frequency behavior of ceramic multilayer capacitors based on device physics is presented. An accurate predictive model incorporating physical dimensions, material constants and aspects of the CMC application environment is presented. This model is suitable for use in the design and development of improved high frequency CMC structures.**

I. Introduction

The physical modelling described in the following is primarily intended for the designer of high frequency ceramic multilayer capacitors (CMC's). Secondarily, users of CMC's can gain insight into the optimal placement of CMC's in their application environment.

Manuscript received September 27, 1991; revised March 10, 1992.

The authors are with the Delft University of Technology, Department of Electrical Engineering, Laboratory for Telecommunication and Remote Sensing Technology, P.O. Box 5031, 2600 GA Delft, The Netherlands.

IEEE Log Number 9200934.

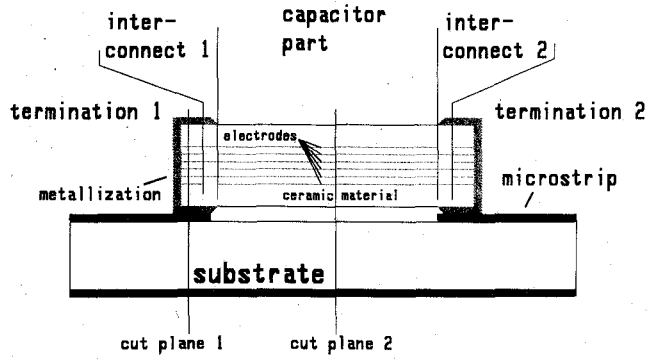

Fig. 1. Cross-section of CMC.

II. The Model

In 1991 Perna proposed a simple resonant folded transmission line model for a CMC mounted in series in a transmission line [1]. In 1987 Ingalls and Kent reexamined Perna's folded line model [2]. They tried to give the model a more rigorous basis and measured devices using the latest VNA's. This study has resulted in a more fundamental predictive model which has subsequently been proven in practice.

The structure under study is that of the intrinsic CMC mounted in an application environment as given in Fig. 1. It is clear from the figure that the capacitor conceptually consists of the following three regions:

The terminations:	connection of the electrodes and the metallization.
The interconnects:	interface between the terminations and the central capacitive region.
The capacitive part:	this is the actual capacitor consisting of a rectangular block of ceramic dielectric in which a number of interleaved precious-metal electrodes have been chosen to yield high capacitance per unit volume.

Transformation to an equivalent circuit model may be made by treating the electrodes and the terminations as multiconductor sections. This requires the accurate calculation of the multiconductor parameters. The device simulator PISCES has been used to carry out these computations [3]. In our case its use is limited to the calculation of the capacitance per unit length between the conductors. These conductors are entered into the program as cross-sections separated by ideal insulating materials whose dielectric constants correspond to those of the CMC under consideration. Solutions are found in a two dimensional plane which somewhat restricts the validity of the model for complicated structures at higher frequencies (i.e. a 100 pF capacitor with 6 plates is accurately modelled up to 10 GHz, a similar 330 pF capacitor model is accurate up to about 9 GHz). This restriction lies in the fact that there are a small number of three dimensional discontinuity regions which can not be accurately calculated in this way.

Keeping these restrictions in mind, we can transform the physical structure into a HF equivalent circuit as shown in Fig. 2. In the capacitive section each electrode is represented by a conductor ref-